

Combining Aggregates of Synthetic Microscale Nanorobots with Swarms of Computer-controlled Flagellated Bacterial Robots to Enhance Target Therapies Through the Human Vascular Network

Sylvain Martel

NanoRobotics Laboratory, Dept. of Computer and Software Engineering, and Institute of Biomedical Engineering,
École Polytechnique de Montréal (EPM), Campus of the Université de Montréal,
Montréal, Canada
E-mail: sylvain.martel@polymtl.ca

Abstract—The field of medical nanorobotics exploits nanometer-scale components and phenomena to enable new or at least to enhance existing medical diagnostic and interventional procedures. The best route for such miniature robots to access the various regions inside the human body is certainly the vascular network which is constituted of nearly 100,000 km of blood vessels. The variations in blood vessels diameters from a few millimeters in the arteries, down to ~4 μm in the capillaries with respective important variations in blood flow velocities, lead to significant challenges in the development of a robot relying on a single type of propulsion method while being trackable in the human body. This tracking feasibility in a living body was realized experimentally by integrating magnetic nanoparticles (MNP) capable of creating a net field inhomogeneity that could be detected by magnetic resonance imaging (MRI). In such an environment, dipole-dipole interaction between synthetic microscale nanorobots encapsulating MNP can be used to achieve higher magnetophoretic velocities when subjected to a 3D magnetic gradient force generated by an upgraded MRI platform to allow such aggregated nanorobots to travel in the blood circulatory network. Nonetheless, the potential limitations of using an artificial approach especially in the human microvasculature suggests that a biological system such as the molecular motors capable of flagellar propelling thrust force exceeding 4 pN provided by each MC-1 MRI-trackable magnetotactic bacteria swimming as swarms under computer control in blood vessels could enhance targeting efficacy in regions such as tumors. Presently, such artificial and natural approaches are unique and very different from any other methods proposed elsewhere. In this paper, these approaches are described with examples of implementations with the goal of demonstrating the potential advantages of combining them for targeting regions deep in the human body.

Keywords—Magnetic nanoparticles; medical nanorobots, magnetic resonance imaging, magnetotactic bacteria, target therapy

I. INTRODUCTION

This paper is based on [1] where synthetic microscale nanorobots were compared to flagellated bacterial robots for target intervention in the human vasculature. Here, not only the main differences in both types are compared but there are described in more details with the goal of demonstrating

the potential advantages of combining artificial or synthetic microscale robots with natural or biological microscale robots for specific target interventions in the human body. But first, as we refer to such untethered entities or agents as robots, the readers must be aware of what this term means in the context of navigable microscale entities in the blood vessels, considering present technological limits.

There are many opinions of what would define a robot. For instance, several organizations including the Robotics Institute of America (RIA) define a robot as a re-programmable multi-functional manipulator designed to move materials, parts, tools, or specialized devices through variable programmed motions for the performance of a variety of tasks. Accordingly, an untethered entity or device capable of programmable motion for the performance of a variety of tasks such as the delivery of therapeutic agents at a specific location in the human body could be viewed as a robot under such a definition. In turn, this definition could be extended to include a microscale robot if its overall dimension would be in the micrometer-range and ideally below 100 μm across. Unlike a nanorobot which can be viewed as a nanometer-scale robot, a microscale nanorobot is defined here as a robot with overall dimensions in the micrometer range that depends on nanometer-scale components (typically less than 100 nm across) to embed characteristics allowing such robot to accomplish its assigned tasks. Embedded magnetic nanoparticles (MNP) can be considered as one type of these components allowing propulsion/steering, tracking, and hyperthermic functions to name but the main ones made possible.

Indeed, MNP can be manipulated by an external magnetic field gradient with the capability of disrupting a high intensity local magnetic field creating a net field inhomogeneity that can be picked up by magnetic resonance imaging (MRI). Such signals can then be fed back to an external computer as tracking data to be processed to perform closed-loop navigation or trajectory control along a pre-planned path.

But present implementations for target interventions using MNP alone have major limitations due to the fact that the approach relies on a permanent (or an electro-magnet) that must be located near the targeted region. The higher

field intensity towards and very near the external magnet restrict targeting to regions near the skin and when the target is located deeper in the human body, a significant reduction of targeting efficacy is expected. When coupled with the fact that the approach relies on trapping the MNP without trajectory servo-control based on tracking information from the release site and towards the target, the approach seems extremely limited. This observation becomes more evident when we look at the distance between the reachable limits of catheterization and targets reachable through complex microvasculature networks such as the ones near a tumor.

Therefore, when operating in the human vascular network, untethered microscale robots capable of performing such tasks must be capable of directional propulsion and/or steering in a 3D volume while being trackable in the body by a suitable imaging modality such as MRI. When these conditions would be met, effective navigation along pre-planned paths through real-time closed-loop control from the release site typically at the catheterization boundaries to as close as possible to a specific target possibly reachable through the microvasculature, would be feasible.

II. TRACKING METHOD

Unlike in the cases of most robotic systems, a tracking approach based on direct-line-of-sight is not possible when operating in the vascular network. Among the few imaging techniques available for such application, X-ray or computed tomography (CT) scan, and MRI stand as the two main potential and widely accepted imaging modalities that are presently widely used in clinics and hospitals.

Since the blood vessels represent the routes to be navigated by these microscale robots, it becomes important to image as many blood vessels that are along the planned path using angiography. Presently, X-ray digital subtraction angiography (DSA) still has the best spatial and temporal resolution for imaging blood vessels. However X-ray has poor soft-tissue information and a high radiation exposure, two disadvantages that do not apply with MRI. As such, substantial research efforts attempt to replace X-ray angiography by magnetic resonance angiography (MRA). Despite the recent progresses in MRA, presently DSA is still the preferred and most appropriate technique to image the vascular network.

The fact that DSA could be used to gather data for the pre-navigation/planning phase of the microscale robots does not mean that X-ray is the most appropriate imaging to gather real-time tracking information of the robots navigating in the blood vessels. This is a critical issue since the spatial resolution of X-ray although better than MRI is still not sufficient to detect such microscale robots when traveling in smaller diameter vessels (e.g. from the small diameter arterioles to the capillaries). On the other hand, MRI-tracking deep in the human body can be achieved with a proper MRI sequence if the magnetic components embedded in such microscale robots create a sufficiently

large local distortion of the magnetic field inside the bore (tunnel) of the MRI scanner. Indeed, the local magnetic field distortion from a magnetic spherical particle for instance can be found at a point P of coordinate $r(x, y, z)$ by that of a magnetic dipole as

$$\vec{B}'(P) = \frac{\mu_0}{4\pi} \left(3 \frac{(\vec{m} \cdot \vec{r}) \vec{r}}{r^5} - \frac{\vec{m}}{r^3} \right). \quad (1)$$

where $\mu_0 = 4\pi \times 10^{-7} \text{ H} \cdot \text{m}^{-1}$ is the permeability of free space such that for a uniformly magnetized object, the dipolar magnetic moment ($\text{A} \cdot \text{m}^2$) depends on the magnetization saturation of the material and is given by

$$\vec{m} = \frac{4}{3} \pi a^3 \vec{M}_{SAT} \quad (2)$$

where a here represents the radius (m) and M_{SAT} being the magnetization saturation of the material used.

Indeed, in [2] we showed that the susceptibility-based negative contrast in MRI can be used to track such magnetic microscale robots with dimensions as small as $15 \mu\text{m}$ in the human body. In this case, the same ferromagnetic material with high susceptibility and used for propulsion was used to induce a perturbation in the main magnetic field homogeneity of a 1.5T clinical MRI scanner. This perturbation can be set during the synthesis process of the microscale robots to reach a level much larger than the robot itself. By creating an artifact from the magnetic material embedded in the microscale robot with a size equivalent or slightly larger than a typical MRI voxel ($\sim 0.5 \times 0.5 \times 0.5 \text{ mm}^3$), the microscale robot will become MRI-trackable.

One method is to use the intra-voxel de-phasing in the Gradient Echo (GE) sequence. This method aims at amplifying the effect of a microscale magnetic object such as a robot that is too small to be visualized in the MR-image or with any other medical imaging modalities.

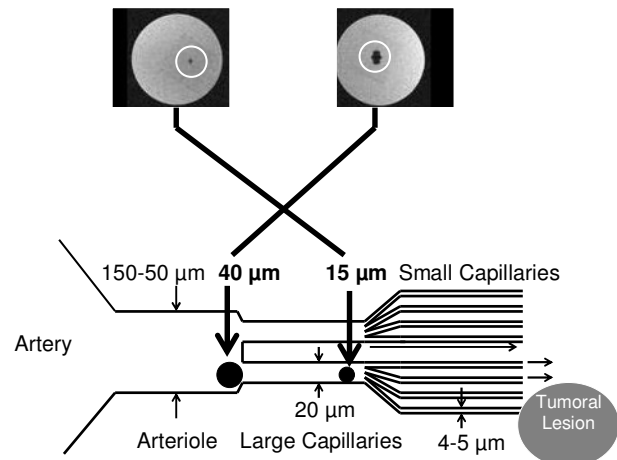


Fig. 1 – Experimental coronal images of a stainless steel bead with an overall diameter of 15 μm imaged using a 1.5 T scanner with a Time Echo (TE) of 30 ms.

III. PROPULSION AND STEERING

A. Single Synthetic Microscale Nanorobot

Even if tracking information is gathered from a modern medical imaging modality such as MRI, propelling and/or steering (when blood flow is used for propulsion) MNP sufficiently to direct them effectively along a pre-planned trajectory is not possible or at least extremely challenging due to the amplitude of magnetic gradients being required. Such required gradient amplitude is presently well beyond technological limitations when operating in some regions of the body of a human adult (e.g. inside the torso) because of the distance separating the MNP from the source generating the directional magnetic gradient field. This is also in great part due to the small volume of MNP even when synthesized with materials having the highest magnetization saturation. This is depicted in Eq. 3.

$$\vec{F}_M = R \cdot V (\vec{M} \cdot \nabla) \vec{B}. \quad (3)$$

The induced magnetic force (N) (Eq. 3) produced by magnetic gradients (T m^{-1}) and acting on a ferromagnetic core with a volume V (m^3), depends on the duty cycle R , i.e. the percentage of time per navigation closed-loop control cycle being dedicated to propulsion (dimensionless) which can be reduced due to longer MRI-tracking acquisition time and/or to allow time for cooling of the coils in particular cases, and the volume magnetization of the core material (A m^{-1}). When such magnetization reaches a saturation level (M_{SAT}), the highest induced propulsion force per unit volume can be reached for a given ferromagnetic material. This would typically be the case when placed in a high intensity magnetic field such as in the bore or tunnel of a standard 1.5T or higher field clinical MRI system. Furthermore, such gradient force unlike the use of an external magnet is constant within the 3D working space inside the bore of MRI systems.

Nonetheless, our initial studies [3] for the development of what we are referring to as a double-insert, i.e. a set of propulsion coils (to increase gradients beyond the 40 mT/m limitation as found in typical clinical MRI systems) that allow MR-imaging to be performed in a time-multiplexed fashion and designed to be installed inside the bore of a clinical MRI system, would still have limited capabilities. This is mainly due to limitation of modern technologies to dissipate the heat generated by such coils. With an inner diameter capable to accommodate a human adult, our initial studies suggest that the maximum gradient amplitude that could be generated would be $\sim 400\text{-}500$ mT/m. It is then obvious as stated earlier and as depicted in Eq. 3 that a directional force sufficient to influence the path of

independent MNP for achieving efficient targeting, cannot be generated for human subjects unless being restricted only to some body's regions such as the legs or arms for instance. For operating in all regions of the human's body (but without transiting through the blood brain barrier (BBB)), this suggests that a cluster or aggregate of MNP with a sufficiently high magnetization saturation level must be encapsulated within a material as to form an entity or robot that could be sufficient to increase effectively V . This would provide an induced magnetic force (Eq. 4) for each robot that would be made of n embedded ferromagnetic cores or superparamagnetic MNP, each with a volume V where $nV \leq V_R$ being the volume of each robot, assuming that all embedded MNP are identical.

$$\vec{F}_{MR} = R \cdot \left(\sum_n V \right) (\vec{M} \cdot \nabla) \vec{B}, \quad nV \leq V_R. \quad (4)$$

Except for transiting through the BBB for targeting inside the brain, such entities do not need to be smaller than approximately half the diameter of the tiniest blood vessels found in humans, i.e. untethered entities should not have an outer diameter much greater than 2 μm and much smaller than 2 μm . Larger diameters would decrease magnetophoretic velocities of such entities in the tiniest vessels due to wall retardation effects while smaller ones would typically lead to a lower charge of magnetic material being embedded. Hence, in order to increase the effective V , a relatively large quantity of MNP can be encapsulated within a non-magnetic material. Such synthetic entity or microscale synthetic robot would then have a magnetophoretic velocity expressed as

$$\overline{v}_M = \frac{\vec{F}_{MR}}{f}. \quad (5)$$

In Eq. 5, f is the friction factor. The value of the friction factor depends on the geometry of the entity being navigated. As stated earlier, the high magnetic field provided by a clinical MRI platform allows us to achieve maximum propulsion force density through magnetization saturation of the MNP while providing an image modality capable of feeding back tracking information to a servo-controller. But when inserted in a high magnetic field, MNP will align to the lines of the magnetic field and maintain the same orientation while operating in such magnetic field. In a clinical MRI system, this homogeneous magnetic field with typical values of 1.5 T or 3.0 T is known as the B_0 field. A spherical shape (lack of anisotropy) would then be a good choice since it would provide a constant friction factor that would be independent of the direction of any navigated blood vessels relative to the B_0 field. As such, the friction factor for such untethered microscale spherical synthetic robot with embedded MNP would be computed as

$$f = 3\pi\eta d_R \cdot \quad (6)$$

In Eq. 6, where η is the viscosity of the medium (e.g. 1.0 mPa·s in water at 20 °C), and d_R is the diameter (m) of the spherical robot. Hence assuming that the synthetic microscale robots would have a spherical shape, Eq. 4 can be re-written as

$$\vec{F}_{MR} = R \cdot \left(p(4/3)\pi d_R^3 \right) (\vec{M} \cdot \nabla) \vec{B}. \quad (7)$$

where p is the percentage of ferromagnetic or superparamagnetic material in each untethered microscale spherical robot.

B. Aggregated Synthetic Microscale Nanorobots

Considering the aforementioned equations, one can easily deduct that a larger untethered robot based on such method of propulsion will have a higher magnetophoretic velocity (if charged with the same percentage of the same type of MNP) than a smaller robot if the diameter of the blood vessel is large enough to avoid wall retardation effects. But smaller robots would be required to travel in smaller diameter vessels.

One solution to this issue is the use of an aggregation of smaller robots. Indeed, the effective V can also be increased with an aggregation of such microscale robots. The level of propulsion/steering force for such aggregation will depend on the coupling force between neighbored robots or untethered entities. When in a high intensity magnetic field, each untethered microscale robot generates a local magnetic dipole. It is this dipole-dipole interaction between neighbored robots that maintains such aggregation. A strong attracting force through strong dipole-dipole interactions between the microscale robots will help maintaining the entities agglomerated while effectively increasing the volume of magnetic material, leading to higher magnetophoretic velocities. But more loosely coupled interactions caused by a lower level of dipole-dipole interactions and/or the use of surfactants or a surface acting like a surfactant (potentially caused by the addition of some types of functionalized molecules), will allow such aggregate to reconfigure when transiting between various vessels geometries such as transiting from larger to smaller diameter vessels. But such lower interactions may result in unexpected or unwanted breakages when encountering obstacles or forces such as the ones created by vortices, which may result in several smaller aggregates, each having lower magnetophoretic velocities than what would be possible with a single larger aggregate. On the other hand, when the interacting forces are too high, an unwanted embolization may occur when transiting from a larger diameter vessel to a smaller one, preventing such aggregate to pursue its course. Therefore, the right compromise in the level of dipole-dipole interacting forces must be set during

the synthesis of such microscale robots, taking into account both physiological and technological characteristics. To help in the design or synthesis of such aggregated microscale synthetic robots, Eq. 8 is used to calculate the dipole-dipole interaction energy E_D between two neighbored robots A and B with respective dipoles μ_A and μ_B . Such interaction depends on not only on the relative orientations of the dipoles but also on their orientation with respect to the vector r_{AB} joining the center of the two dipoles.

$$E_D = -\frac{\mu_0}{4\pi} \left(\frac{(\mu_A \cdot r_{AB})(\mu_B \cdot r_{AB})}{r_{AB}^5} - \frac{\mu_A \cdot \mu_B}{r_{AB}^3} \right), r_{AB} = \|r_{AB}\| \quad (8)$$

Since the lowest energy configuration corresponds to the two magnetic moments aligned head-to-tail, neighbored (i.e. closed enough for E_D to be non-negligible) microscale synthetic robots when in a MRI system, will tend to form needle-like aggregates with an elongated axe being oriented in the direction of the B_0 field. This phenomenon is taken into consideration with regard to the angle between the B_0 field and directional motion of the aggregate.

C. Self-propelled Bacterial Nanorobots

A self-propelled entity refers here as an entity that can propel itself without any propulsion force produced by an external source. Flagellated bacteria and more specifically magnetotactic bacteria (MTB) [4] acting under computer control can be described as self-propelled nanorobots [5] since they rely on nanometer-scale components to act as a robot. One example is the chain of magnetite nanoparticles (magnetosomes) embedded in the cell of the MTB. Such chain can act as a miniature magnetic compass needle [6]. When a directional torque is induced on such a chain from an electro-magnetic field under computer control, precise directional control of polar MTB can be achieved. This is referred here to as magnetotaxis [7] control. Our studies showed that the MC-1 MTB is presently the most appropriate bacteria for such target applications. The same magnetosomes can also be used for tracking purpose as explained in Eq. 1. The self-propulsion system of each bacterium in the form of two flagellar bundles allows efficient propulsion in low Reynolds regime without the limitation of gradient forces generated from an external source.

IV. BACTERIAL PROPULSION – EXPERIMENTAL RESULTS

The advantage of bacterial propulsion over the gradient-based propulsion mentioned earlier becomes evident in low Reynolds regime and in the microvasculature. Again, from Stokes equation, we have a thrust force (N) provided by the two flagellar bundles on the back of the spherical cell with a radius a_B (m) being calculated from observed terminal velocities as

$$\vec{F}_T = \frac{\vec{v}_T}{3\pi\eta a_B} \quad (7)$$

From swimming velocities of the MC-1 cells recorded in water at room temperature, the thrust force was estimated at more than 4.0 pN (~10 times the thrust force provided by other well known species of flagellated bacteria). To reach the tumoral lesion, capillaries with a diameter as small as ~4 μm can be expected. Hence, the maximum radius of a spherical synthetic microscale robot would be limited by the wall retardation effect being expressed as

$$\frac{v}{v_\infty} = \left(\frac{1-\lambda}{1-0.475\lambda} \right)^4 \quad (8)$$

where v and v_∞ is the velocity of the spherical synthetic robot or the MC-1 bacterium in the capillary and in open space respectively, and $\lambda = d/d_C$ which is the ratio between the diameter of the synthetic robot or the cell of the MC-1 bacterium and the inner diameter of the capillary respectively. In the capillaries, the optimal ratio for an untethered synthetic microscale robot propelled by magnetic gradient is ~0.5. Hence, for the smallest diameter capillaries $d_C = 4 \times 10^{-6}$ m, the largest synthetic microscale spherical robot would have $a_R = 1 \times 10^{-6}$ m. To maximize the effective volume of magnetic material being embedded, V_R needs to be maximized while maintaining the ratio at ~0.5, which suggests that $\min a_R = 1 \times 10^{-6}$ m since nothing is gained with a smaller volume except for transiting through the BBB. Considering Eq. 7, when loaded with 100% FeCo MNP for achieving maximum magnetization saturation level, it is obvious that a single synthetic nanorobot with a diameter of 2 μm for travelling in the tiniest blood vessels with the limitation in generating magnetic gradients at the human scale would be much less effective than the minimum thrust force of 4 pN provided by a single 1 to 2- μm in diameter MC-1 MTB. But our preliminary results suggest that when operating in the vascular network at body temperature, unlike for a synthetic version, their motility after a period of time t (in minutes) and hence their swimming speed will be affected according to Eq. 9.

$$v_{B37} = 0.09 t^2 - 8.10 t + v_{MTB} \quad (9)$$

where the initial average swimming velocity $v_{MTB} = 187.85$ $\mu\text{m/s}$ prior to be injected in blood. Hence, the advantage of this particular type of bacterial propulsion is true but of a limited time (approx. 40 minutes) especially in the microvasculature where V is limited due to space constraints and where the formation of aggregates is not possible. On the other hand, our studies showed that in larger vessels especially in arteries and in larger arterioles, synthetic microscale nanorobots will perform better since thrust force above the bacterial thrust force can be achieved.

V. BACTERIAL STEERING

Unlike the synthetic microscale robots that require higher gradients as their volume decreases in order to induce a sufficiently high propulsion/steering force for targeting or navigation purpose, the fact that the magnetic field for a polar MTB is only used for directional control and not to provide a propelling force, translates into the need for a much lower magnitude of magnetic field with makes the navigation of smaller untethered robots in the human body, technologically possible using much less power. Indeed, the magnetotactic bacteria of type MC-1 and depicted in Fig. 2 is an example of a biological microscale robot where the flagella bundles are the propulsion (propulsive) system and the chain of membrane-based nanoparticles known as magnetosomes embedded in the cell implements an embedded steering system by acting like a miniature magnetic compass needle that can be oriented by inducing a torque from a directional magnetic field.

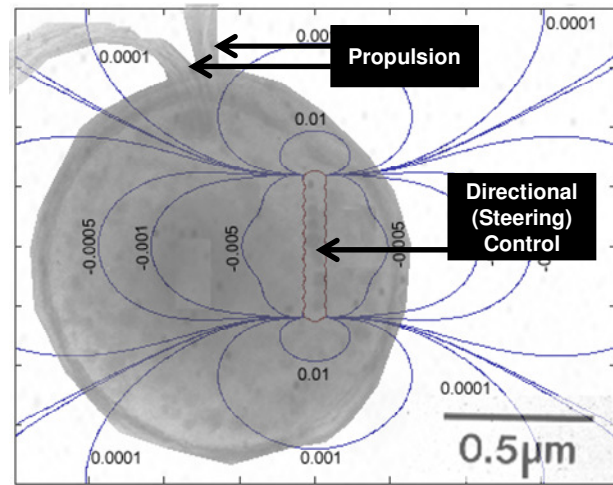


Fig. 2 – Electron photograph of a MC-1 magnetotactic bacterium acting as a biological microscale robot with the two flagella bundles and the chain of magnetosomes used for propulsion and steering respectively.

Indeed, here directional control is performed by inducing a directional torque T by applying a directional magnetic field B as described by the following equation:

$$\vec{T} = V \cdot \vec{M} \times \vec{B} \quad (10)$$

Since for a robot with the same volume and magnetization, the magnitude of the magnetic field required is much less for generating a directional torque compared to a directional displacement (propulsion) force, directional control of such robot capable of providing its own propulsion (propelling) force would require significantly less power.

VI. COMBINING MAGNETIC AND BACTERIAL PROPULSIONS

Many targets such as tumoral lesions located deeper in the body can be accessed by travelling through a microvascular network including the angiogenesis network. But because of the size of the blood vessels, the injection process is typically performed in larger diameter vessels, typically in an artery. As such, combining magnetic-based propulsion with self-propelled bacterial carriers can lead to enhanced targeting efficacy when travelling through the microvasculature is essential, which is most often the case in tumor targeting. Indeed, since bacterial propulsion based on the MC-1 MTB has a minimum thrust force of 4 pN which is approximately 10 times the thrust force that has been measured for other well known species of flagellated bacteria, suggests that it could be used as a complementary means of propulsion when targeting deep in the vasculature. In other words, such bacterial propulsion may become more effective at a location where magnetic propulsion becomes ineffective since it does not rely on an external source as magnetic propulsion does. The latter can be explained as stated earlier by the fact that the smaller diameters of the blood vessels prevent the use of synthetic microscale nanorobots with a sufficiently large volume of embedded magnetic material for sufficient propulsion within known technological limitations.

But there is another important advantage of using such flagellated bacteria when operating in the microvasculature. Indeed, such bacterial robots have what is referred to here as path finding (PF) capability. When a directional magnetic field is used (outside the tunnel of a MRI scanner) to point in the desired direction of motion for the bacterial robots (e.g. towards a target such as a tumor), the latter will move under the influence of the induced torque generated by the same directional field. When a MTB reaches a sufficiently wide obstacle (which is often the case in the microvasculature, e.g. vessel's walls), it will not typically remain at the location where it reached the obstacle as a synthetic microrobot will until the direction of the magnetic field is changed but instead, it will look for a path that will lead toward the direction of the magnetic field. Since the small blood vessels found in the microvasculature cannot presently be imaged due to a lack of spatial resolution of all existing medical imaging modalities, knowing in which direction the induced force should be applied to navigate synthetic microscale robots in such chaotic maze of blood vessels without such image information is practically not possible. This is why the use of bacterial microscale robots can make a huge difference in targeting efficacy when operating in such physiological environments.

Nonetheless, to take advantage of this PF capability as well as the enhanced propulsive force provided by MTB in the microvasculature, such bacteria loaded with therapeutic agents must be carried from the catheterization boundary in an artery to the entry of the microvascular network. As such, special micro-carriers based on magnetic propulsion and

capable of encapsulating such MTB must be used. The general concept is depicted in Fig. 3.

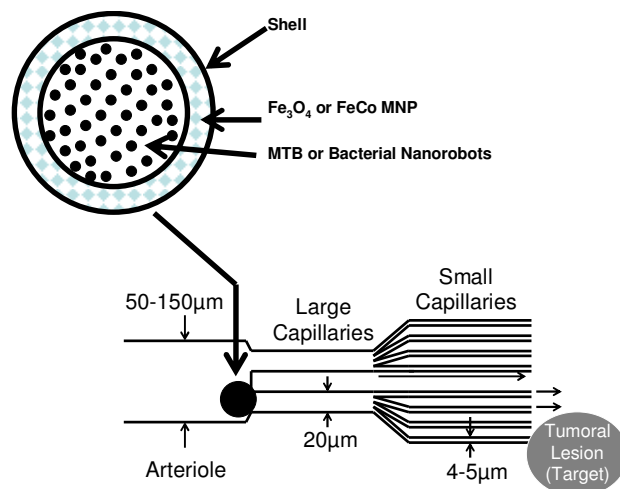


Fig. 3 – Diagram showing the general concept of encapsulating MTB to transport them towards the microvasculature

The synthesis of such carriers with various diameters down to approximately 10 µm and containing MC-1 bacteria capable of free swimming inside the shell as depicted in Fig. 3 has been done successfully by our research group. But more experimental data needed to be recorded before we can validate the idea of transporting drug-loaded MTB. Nonetheless, preliminary experimental results suggest that this concept is very promising.

VII. REDUCTION OF THE BLOOD FLOW

Another complementary strategy that may enhance targeting in deep regions is to increase the effective propulsive force of MTB in the microvasculature by reducing temporarily the blood flow with the use of synthetic polymorphic microscale robots. Polymorphic microscale robots have the ability to change forms or volumes. For instance, such a robot could travel in a specific blood vessel with a lower overall volume and use a higher volume to create a temporary embolization at a specific site that would eliminate or at least reduce the blood flow to help the MTB navigating more efficiently.

Our first prototypes [8] of such polymorphic microscale robots were made of biocompatible N-isopropylacrylamide (PNIPA) hydrogel. Such hydrogel reduces its size in response to an elevation of temperature above a specific threshold. This temperature threshold referred to as the lower critical solution temperature (LCST) is adjusted slightly above 37°C by the addition of several monomers. The local heat responsible to trigger the volume change is generated by biocompatible ~20 nm single-domain superparamagnetic Iron-Oxide (Fe₃O₄) MNP (the use of FeCo MNP could also be envisioned) embedded into the

PNIPA structure and are also used for propulsion and steering. The characteristics of these MNP are adjusted to allow the energy from a magnetic field to drive the magnetic moments capable of overcoming the thermal energy barrier and to allow a rotation and an alignment with the direction of the same magnetic field. After removing the external magnetic field, magnetic moments do not relax immediately, but after a short delay before returning to their original random orientation. During this process known as the Néel relaxation, energy is released in the form of heat that is used to rise the temperature inside the hydrogel-based microscale robot. Several microscale polymorphic robots were tested successfully using a 4 kA.m^{-1} magnetic field modulated at 160 kHz. This approach is summarized schematically in Fig. 4.

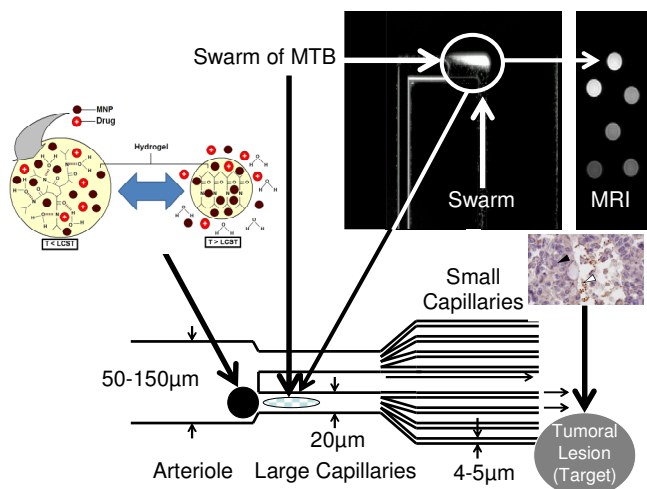


Fig. 4 – Schematic of the use of polymorphic microscale robots to reduce the blood flow in order to enhance targeting using a swarm of bacterial microscale robots

VIII. CONCLUSION

An aggregate of synthetic microscale robots will have higher propulsion performance in larger vessels. On the other hand, MC-1 bacterial propulsion proves to be superior in the microvasculature. Combining both approaches should lead to optimum targeting performance in regions located deeply in the human vascular network. One promising approach presented here is to encapsulate self-propelled bacteria acting as biological microscale robots operating under the control of an external computer into special micro-carriers being propelled by magnetic gradients produced by an upgraded MRI scanner. This combination allow complementary propulsion methods necessary to target more efficiently specific regions located deeper and accessible by transiting through the microvasculature after being introduced in the body through an artery. Another

complementary approach is based on polymorphic synthetic microscale robots capable of changing volume to produce temporary embolization that would allow a reduction of the blood flow in smaller diameter capillaries and hence, potentially help achieving enhanced targeting efficacy. Although more types of microscale robots could be envisioned, this paper already showed the potential advantages of combining aggregates of synthetic and biologic microscale robots for specific medical interventions such as in cancer therapies.

ACKNOWLEDGMENT

This project is supported in part by the Canada Research Chair (CRC) in Micro/Nanosystem Development, Fabrication and Validation and grants from the National Sciences and Engineering Research Council of Canada (NSERC), the Province of Québec, the Canada Foundation for Innovation (CFI), and US Grant Number R21EB007506 from the National Institute Of Biomedical Imaging And Bioengineering. The content is solely the responsibility of the authors and does not necessary represent the official views of the National Institute Of Biomedical Imaging And Bioengineering or the National Institutes of Health.

REFERENCES

- [1] S. Martel, "Aggregates of synthetic microscale nanorobots versus swarms of computer-controlled flagellated bacterial robots for target therapies through the human vascular network," *The Fourth Int. Conf. on Quantum, Nano and Micro Technologies (ICQNM 2010)*, St. Marteen, Netherlands Antilles, Feb. 10-16, 2010
- [2] N. Olamaei, G. Beaudoin, G. Cheriet and S. Martel, "MRI visualization of a single 15 µm navigable imaging agent and future microrobot," *32nd Annual International Conference of the IEEE Engineering in Medicine and Biology Society (EMBC)*, Buenos Aires, Argentina, Aug. 31 – Sept. 4, 2010
- [3] S. Martel, O. Felfoul, J.B. Mathieu, A. Chanu, S. Tamaz, M. Mohammadi, M. Mankiewicz, and N. Tabatabaei, "MRI-based nanorobotic platform for the control of magnetic nanoparticles and flagellated bacteria for target interventions in human capillaries," *International Journal of Robotics Research (IJRR), Special Issue on Medical Robotics*, vol. 28, no. 9, pp. 1169-1182, Aug. 2009
- [4] R. P. Blakemore, "Magnetotactic bacteria," *Science*, 190, pp. 377-379, 1975
- [5] S. Martel, M. Mohammadi, O. Felfoul, Z. Lu, and P. Poupponneau, "Flagellated magnetotactic bacteria as controlled MRI-trackable propulsion and steering systems for medical nanorobots operating in the human microvasculature," *International Journal of Robotics Research (IJRR)*, vol. 28, no. 4, pp. 571-582, April 2009
- [6] R. B. Frankel and R. P. Blakemore, "Navigational compass in magnetic bacteria," *J. of Magn. and Magn. Materials*, 15-18 (3), pp. 1562-1564, 1980
- [7] H. Debarros, D. M. S. Esquivel, and M. Farina, "Magnetotaxis," *Sci. Progr.*, 74, pp. 347-359, 1990
- [8] N. Tabatabaei, J. Lapointe and S. Martel, "Microscale hydrogel-based computer-triggered polymorphic microrobots for operations in the vascular network," *3rd IEEE RAS EMBS Int. Conf. on Biomedical Robotics and Biomechatronics (BioRob)*, Tokyo, Japan, Sept. 26-30, 2010